J. Fluid Mech. (1995), vol. 305, pp. 263–279

Scattering by a periodic array of rectangular blocks

By M. FERNYHOUGH AND D. V. EVANS
School of Mathematics, University of Bristol, Bristol BS8 1TW, UK

(Received 15 May 1995)

Scattering properties of an incident field upon a periodic array of identical rectangular barriers, each extending throughout the water depth, are calculated based on a Galerkin approximation to an integral representation of the problem derived using the linear theory of water waves. The method incorporates full multi-modal scattering using a matrix formulation and is equivalent to a corresponding two-dimensional acoustics problem also discussed.

1. Introduction

In a recent paper by Porter & Evans (1995), a possible scheme for a breakwater was considered which consisted of a periodic array of thin-walled barriers in the form of identical vertical barriers extending throughout the water depth. Using classical linear water wave theory they separated out the depth dependence and reduced the problem to solving the two-dimensional Helmholtz equation, which is identical to a problem in linear acoustics, optics or electromagnetism involving an equivalent diffraction grating. They were able to obtain extremely accurate complementary bounds to the solution and include multi-modal scattering. Other authors who have considered this problem are Dalrymple & Martin (1990) and Williams & Crull (1993), the latter exploiting a technique used by Achenbach & Li (1986) for a general orientation of the barriers.

A similar problem in acoustic scattering was also considered by Linton & Evans (1993*a*) but in this case the barriers were rotated through an angle $\pi/2$ to form an array of parallel plates. They showed that an accurate approximate solution could be obtained by relating the full problem to two simpler problems, each of which could be solved explicitly using a residue calculus technique. However the method was restricted to single mode scattering. There exists an enormous amount of literature on the general theory of gratings. See for example Petit (1980) and Wilcox (1984) for a detailed discussion and extensive bibliographies.

In this paper we consider the multi-modal scattering properties of an incident field upon a periodic array of rectangular blocks using ideas developed in Evans & Fernyhough (1995) hereafter denoted by I, where we provided numerical evidence of edge waves travelling along a periodic coastline consisting of a straight and vertical cliff-face with protruding rectangular barriers. The assumption that the water depth is constant again reduces the problem to the two-dimensional Helmholtz equation with analogies in acoustics for example, as in the papers described above.

The rectangular geometry invites an approach based on enforcing the continuity of appropriate eigenfunction expansions resulting in infinite systems of equations for the unknown Fourier coefficients in the expansions in each region. Many authors have used this approach for related problems, and have obtained the coefficients by truncation of the infinite system. Thus Mongeau, Amram & Rousselet (1986) used this method to consider the scattering of sound waves by a periodic array of slotted waveguides, extending the work of Kristiansen & Fahy (1972). This approach can be criticised on two counts. First the systems obtained are usually slowly convergent since the eigenfunctions are required to model the behaviour of the flow near the sharp corners of the blocks where the flow velocity is unbounded. Secondly, there is usually no guarantee that the truncated system converges to the solution of the infinite system as the truncation parameter increases indefinitely.

Here we proceed differently. Rather than solve the infinite system directly, we formulate the problem in terms of integral equations having positive kernels and identify the important reflection and transmission coefficients as integrals of the solutions to these equations described by the elements of certain matrices. A Galerkin approximation is then sought using expansion functions which correctly model the singularities at the edges of the blocks in a similar fashion to I, and which provide the maximum simplification of the results. It turns out that extremely efficient results can be obtained with no more than five expansion functions to give at least three-figure accuracy. In the formulation of the matrix system we also show that the energy conservation condition is automatically satisfied from the final form of the reflection vector. The problem is formulated and the matrix system derived in §2.

In §3 we provide results for various geometries of the blocks, wave frequency and angle of incidence of the incoming wave. We also recover the geometries of Porter & Evans (1995) and Linton & Evans (1993*a*) for in-line and parallel plates respectively by 'squashing' the rectangular blocks in the required direction, and obtain excellent agreement. We show a comparison with results from scattering by an infinite row of circular cylinders by Linton & Evans (1993*b*).

2. Formulation and solution

Equations and boundary conditions

Cartesian coordinates are chosen with the rectangular blocks extending throughout the water depth h. Thus the free surface is at $z = 0$, the sea-bed at $z = -h$ and the blocks are equally spaced as shown in figure 1, and positioned symmetrically with respect to the y-axis. The distance between the centre of adjacent blocks is d. The length of each block is $2a$ and width $c = d - b$. Because the blocks extend throughout the depth it is possible to extract the z-dependence from the linearized velocity potential $\Phi(x, y, z, t)$ describing the motion. In addition we assume a time-harmonic motion of frequency $\omega/2\pi$ so that

$$\Phi(x, y, z, t) = \mathrm{Re}\left\{\phi(x, y)\cosh k(z + h)\,\mathrm{e}^{-\mathrm{i}\omega t}\right\}, \tag{2.1}$$

where k is the real root of

$$\omega^2 = gk \tanh kh. \tag{2.2}$$

In the context of acoustics (2.2) is replaced by

$$\omega = kc_v \tag{2.3}$$

where c_v is the velocity of sound.

On the basis of either linear acoustics or water waves we seek solutions to the

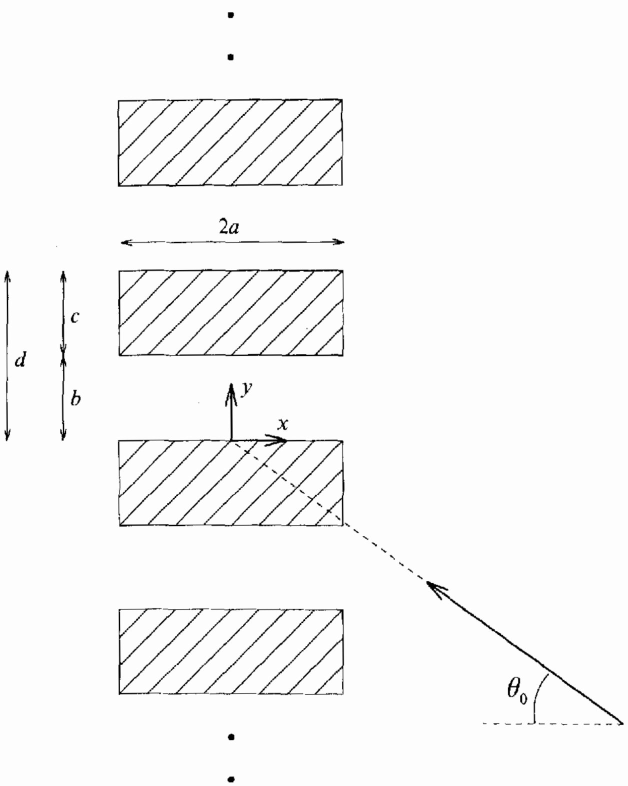

FIGURE 1. Periodic rectangular arrays.

two-dimensional Helmholtz equation

$$\frac{\partial^2 \phi}{\partial x^2} + \frac{\partial^2 \phi}{\partial y^2} + k^2 \phi = 0 \tag{2.4}$$

in the fluid, and

$$\frac{\partial \phi}{\partial n} = 0 \tag{2.5}$$

on the boundaries of each block.

We assume an incident wave from $x > a$ of the form

$$\phi_i(x, y) = \mathrm{e}^{-\mathrm{i}k(x \cos \theta_0 - y \sin \theta_0)}, \tag{2.6}$$

having wavelength $\lambda = 2\pi/k$ and making an angle $\pi - \theta_0$ with the positive x-direction, $0 \leqslant \theta_0 < \pi/2$.

Equation (2.6) may also be written

$$\phi_i(x, y) = \mathrm{e}^{-\mathrm{i}(\alpha_0 x - \beta_0 y)}, \tag{2.7}$$

where $\beta_0 = k \sin \theta_0$, $\alpha_0 = k \cos \theta_0$.

As in I, the periodicity d of the blocks shows that the fluid at $y + d$ can only differ from the field at y by a factor $\mathrm{e}^{\mathrm{i}\beta_0 d}$, being the shift in phase of the incident wave. This enables us to write

$$\phi(x, y + md) = \mathrm{e}^{\mathrm{i}m\beta_0 d} \phi(x, y), \quad m = 0, \pm 1, \pm 2, \ldots, \tag{2.8}$$

which for $x \geqslant a$ is satisfied by

$$\phi(x, y) = \mathrm{e}^{\mathrm{i}\beta_0 y}\psi(x, y) \tag{2.9}$$

where $\psi(x, y)$ is periodic in y with period d. Equation (2.8) provides the extension of the solution outside the region $y \in [0, d]$.

The most general form for $\phi(x, y)$ satisfying (2.9) is

$$\sum_{n=-\infty}^{\infty} A_n \mathrm{e}^{-\mathrm{i}(\alpha_n x - \beta_n y)}, \tag{2.10}$$

where

$$\beta_n = \beta_0 + \frac{2n\pi}{d} = k \sin\theta_n, \tag{2.11}$$

say, and

$$\alpha_n = \left(k^2 - \beta_n^2\right)^{1/2}. \tag{2.12}$$

We may write (2.11) as

$$\sin\theta_n = \sin\theta_0 + \frac{n\lambda}{d}, \tag{2.13}$$

which has pairs of real solutions θ_n, $\pi - \theta_n$, corresponding to waves travelling in directions symmetric about the line $x = 0$. The precise number of real solutions depends upon λ/d and θ_0.

In general we have $N = r + s + 1$ real solutions with

$$-r \leqslant n \leqslant s \tag{2.14}$$

where

$$r = \left[(1 + \sin\theta_0)\frac{d}{\lambda}\right] \tag{2.15}$$

and

$$s = \left[(1 - \sin\theta_0)\frac{d}{\lambda}\right] \tag{2.16}$$

and $[x]$ denotes the integer part of x.

Note that for

$$\frac{\lambda}{d} > 1 + \sin\theta_0 \tag{2.17}$$

the only real solutions are θ_0 and $\pi - \theta_0$ and there will be a single reflected and transmitted wave.

We define

$$\gamma_n = \begin{cases} (\beta_n^2 - k^2)^{1/2}, & \beta_n > k, \\ -\mathrm{i}(k^2 - \beta_n^2)^{1/2} = -\mathrm{i}\alpha_n, & \beta_n < k. \end{cases} \tag{2.18}$$

From the symmetry in x, it is possible to express $\phi(x, y)$ as

$$\phi(x, y) = \tfrac{1}{2}\left(\phi_s(x, y) + \phi_a(x, y)\right), \tag{2.19}$$

where $\phi_s(\phi_a)$ is even(odd) in x so that

$$\frac{\partial\phi_s}{\partial x} = 0, \quad \phi_a = 0, \quad x = 0, \quad md < y < md + b \quad (m = 0, \pm 1, \pm 2, \ldots). \tag{2.20}$$

The decomposition (2.19) enables us to solve for two separate functions ϕ_s , ϕ_a in

$x \geqslant 0$ only, the extension to $x \leqslant 0$ being through use of

$$\phi_s(-x, y) = \phi_s(x, y) \quad \text{and} \quad \phi_a(-x, y) = -\phi_a(x, y). \tag{2.21}$$

We shall consider in detail the problem for ϕ_s and then describe the slight changes needed in obtaining ϕ_a.

Solution in the outer region

From the preceding subsection $\phi_s(x, y)$ satisfies (2.4), (2.5), (2.20) and appropriate conditions at $x = +\infty$. The most general form of solution in $x \geqslant a$ satisfying (2.4), (2.8) is

$$\phi_s(x, y) = e^{\gamma_0(x-a)}\Psi_0(y) + \sum_{n=-\infty}^{\infty} A_n e^{-\gamma_n(x-a)}\Psi_n(y) \tag{2.22}$$

where

$$\Psi_n(y) = e^{i\beta_n y}, \quad \beta_n = \beta_0 + \frac{2n\pi}{d} \tag{2.23}$$

satisfies

$$\frac{1}{d}\int_0^d \Psi_m(y)\overline{\Psi_n(y)}dy = \delta_{mn} \tag{2.24}$$

and the bar denotes complex conjugate.

We have

$$\gamma_n = (\beta_n^2 - k^2)^{1/2} > 0 \quad \text{for} \quad k < \beta_n \tag{2.25}$$

and we define $\gamma_n = -i\alpha_n$ for $n = -r, -r+1, \ldots, s$ so that there are $r + s + 1$ reflected waves in general, where r, s satisfy (2.15) and (2.16).

Solution in the inner region

For $0 \leqslant x \leqslant a$, $0 \leqslant y \leqslant b$, the solution satisfying (2.4), (2.5), (2.20) is

$$\phi_s(x, y) = \sum_{n=0}^{\infty} B_n \cosh(q_n x)\psi_n(y), \tag{2.26}$$

where

$$\psi_n(y) = \varepsilon_n^{1/2}\cos(p_n y), \quad p_n = \frac{n\pi}{b}, \quad \varepsilon_0 = 1, \quad \varepsilon_n = 2, \quad n > 0$$

and

$$q_n = \begin{cases} (p_n^2 - k^2)^{1/2}, & k \leqslant p_n, \\ -i(k^2 - p_n^2)^{1/2} = -ik_n, & k > p_n, \end{cases} \tag{2.27}$$

satisfying

$$\frac{1}{b}\int_0^b \psi_m(y)\psi_n(y)dy = \delta_{mn}. \tag{2.28}$$

The solution $\phi_s(x, y + md)$ is obtained from (2.26) by inserting the factor $e^{im\beta_0 d}$ on the right-hand side, so as to satisfy (2.8).

For $k > p_n$ there are wave terms in (2.26) involving $\cos(k_n x)$. The number of such terms is given by $M = [2b/\lambda] + 1$, there being just one such term, $\cos(kx)$, if $\lambda > 2b$. It can be seen from (2.14)–(2.16) that the precise values for M, N depend on the parameters λ/d, λ/b and θ_0. However if $\lambda > 2d \geqslant 2b$ it follows from (2.17) that $M = N = 1$ and there is just one reflected wave and one wave travelling along $0 \leqslant y \leqslant b$, $0 \leqslant x \leqslant a$.

Continuity conditions

We need to apply conditions of continuity to ϕ_s and $\partial\phi_s/\partial x$ at $x = a$, $0 \leqslant y \leqslant b$ and to satisfy $\partial\phi_s/\partial x = 0$, $x = a$, $b \leqslant y \leqslant d$. Once this is done the solution will apply for all y because (2.8) is satisfied.

From (2.22) and (2.26) in $0 \leqslant y \leqslant b$

$$\left.\frac{\partial \phi_s}{\partial x}\right|_{x=a} \equiv U(y) = -\sum_{n=-\infty}^{\infty} \gamma_n (A_n - \delta_{n0}) \Psi_n(y) \tag{2.29}$$

$$= \begin{cases} \sum_{n=0}^{\infty} q_n B_n \sinh(q_n a) \psi_n(y), & y \in L_g, \\ 0, & y \in L_b, \end{cases} \tag{2.30}$$

where $L_g : \{x = a, 0 \leqslant y \leqslant b\}$ and $L_b : \{x = a, b \leqslant y \leqslant d\}$.

We first multiply (2.29) by $\overline{\Psi_m(y)}$ and integrate over $[0, d]$ using (2.24) to obtain

$$-\gamma_n d(A_n - \delta_{n0}) = \int_{L_g} U(y) \overline{\Psi_n(y)} \mathrm{d}y. \tag{2.31}$$

Again, multiplying (2.30) by $\psi_m(y)$ and integrating over L_g gives

$$q_n b B_n \sinh(q_n a) = \int_{L_g} U(y) \psi_n(y) \mathrm{d}y. \tag{2.32}$$

Continuity of ϕ_s on L_g now requires, from (2.22) and (2.26), that

$$\sum_{n=-\infty}^{\infty} (A_n + \delta_{n0}) \Psi_n(y) = \sum_{n=0}^{\infty} B_n \cosh(q_n a) \psi_n(y). \tag{2.33}$$

Reformulation with a positive definite operator

At this stage we could substitute for A_n, B_n in (2.33) using (2.31) and (2.32) to derive an integral equation for $U(y)$. This could be solved numerically and the coefficients A_n, B_n then determined from (2.31) and (2.32). However the kernel is not positive definite and the many attractive features of positive definite operators will be lost. We will use a Galerkin approximation and make use of lower bound properties of approximate solutions, so at the cost of some increase in algebra we proceed as follows.

The A_n for $n = -r, -r+1, \ldots, s$, correspond to amplitudes of reflected waves in $x \geqslant a$. To emphasize their prominence we write $A_n = R_n$, $n = -r, -r+1, \ldots, s$. Similarly the B_n for $n = 0, 1, \ldots, M-1$, correspond to amplitudes of wave-like terms in $0 \leqslant x \leqslant a$ which, whilst not having the physical significance of the R_n, prevent the kernel from being positive definite. Thus we substitute for all the A_n in (2.33) using (2.31) except $n = -r, -r+1, \ldots, s$ and for all the B_n in (2.33) using (2.32) except $n = 0, 1, \ldots, M-1$ to obtain

$$\sum_{n=-r}^{s} (R_n + \delta_{n0}) \Psi_n(y) - \sum_{n=0}^{M-1} B_n \cos(k_n a) \psi_n(y) = \int_{L_g} U(t) K(y, t) \mathrm{d}t, \tag{2.34}$$

where

$$K(y, t) = \sum_{n=-\infty}^{\infty}{}' (\gamma_n d)^{-1} \Psi_n(y) \overline{\Psi_n(t)} + \sum_{n=M}^{\infty} (q_n b)^{-1} \coth(q_n a) \psi_n(y) \psi_n(t) \tag{2.35}$$

and the notation $\sum'$ means that the terms $n = -r, -r+1, \ldots, s$ have been omitted.

Let $u_n(y)$, $v_n(y)$ satisfy

$$\int_{L_g} u_n(t)K(y,t)\mathrm{d}t = \Psi_n(y), \;\; y \in L_g \;\; (n = -r, -r+1, \ldots, s) \tag{2.36}$$

and

$$\int_{L_g} v_n(t)K(y,t)\mathrm{d}t = \psi_n(y), \;\; y \in L_g \;\; (n = 0, 1, \ldots, M-1). \tag{2.37}$$

Then

$$U(y) = \sum_{n=-r}^{s} (R_n + \delta_{n0})u_n(y) - \sum_{n=0}^{M-1} B_n \cos(k_n a)v_n(y) \tag{2.38}$$

satisfies (2.34).

We introduce the inner product notation

$$(u, v) = \int_{L_g} u(y)\overline{v(y)}\mathrm{d}y \quad \left(= \overline{(v, u)}\right) \tag{2.39}$$

where the bar denotes complex conjugate, and define the matrices $\mathbf{S}^{(1)}_{(N\times N)}$, $\mathbf{S}^{(2)}_{(N\times M)}$, $\mathbf{S}^{(3)}_{(M\times N)}$, $\mathbf{S}^{(4)}_{(M\times M)}$, where

$$S^{(1)}_{mn} = (u_n, \Psi_m), \;\; S^{(2)}_{mn} = (v_n, \Psi_m), \;\; S^{(3)}_{mn} = (u_n, \psi_m), \;\; S^{(4)}_{mn} = (v_n, \psi_m). \tag{2.40}$$

Then substituting (2.38) into (2.31) gives

$$\mathrm{i}\alpha_n d(R_n - \delta_{n0}) = \sum_{m=-r}^{s} (R_m + \delta_{m0})S^{(1)}_{nm} - \sum_{m=0}^{M-1} B_m \cos(k_m a)S^{(2)}_{nm}, \quad n = -r, -r+1, \ldots, s \tag{2.41}$$

and substituting (2.38) into (2.32) gives

$$-k_n b B_n \sin(k_n a) = \sum_{m=-r}^{s} (R_m + \delta_{m0})S^{(3)}_{nm} - \sum_{m=0}^{M-1} B_m \cos(k_m a)S^{(4)}_{nm}, \quad n = 0, 1, \ldots, M-1. \tag{2.42}$$

Define

$$\mathbf{D}^{(1)} = \mathrm{diag}\{\alpha_n d\}, \;\; n = -r, -r+1, \ldots, s, \tag{2.43}$$

$$\mathbf{D}^{(2)} = \mathrm{diag}\{\cos(k_n a)\}, \;\; n = 0, 1, \ldots, M-1, \tag{2.44}$$

$$\mathbf{D}^{(3)} = \mathrm{diag}\{k_n b \sin(k_n a)\}, \;\; n = 0, 1, \ldots, M-1, \tag{2.45}$$

$$\boldsymbol{U}^T = (0, \ldots, 0, 1, 0, \ldots, 0), \;\; N \text{ terms, } 1 \text{ at zeroth place}, \tag{2.46}$$

$$\boldsymbol{R}^T = (R_{-r}, R_{-r+1}, \ldots, R_s), \;\; N \text{ terms}, \tag{2.47}$$

and

$$\boldsymbol{B}^T = (B_0, B_1, \ldots, B_{M-1}), \;\; M \text{ terms}. \tag{2.48}$$

Then (2.41) and (2.42) may be written as

$$\mathrm{i}\mathbf{D}^{(1)}(\boldsymbol{R} - \boldsymbol{U}) = \mathbf{S}^{(1)}(\boldsymbol{R} + \boldsymbol{U}) - \mathbf{S}^{(2)}\mathbf{D}^{(2)}\boldsymbol{B} \tag{2.49}$$

and

$$-\mathbf{D}^{(3)}\boldsymbol{B} = \mathbf{S}^{(3)}(\boldsymbol{R} + \boldsymbol{U}) - \mathbf{S}^{(4)}\mathbf{D}^{(2)}\boldsymbol{B}, \tag{2.50}$$

from which $\boldsymbol{B}$ can be eliminated to give $\boldsymbol{R}$ as

$$\boldsymbol{R} = -(\mathbf{C} - \mathrm{i}\mathbf{D}^{(1)})^{-1}(\mathbf{C} + \mathrm{i}\mathbf{D}^{(1)})\boldsymbol{U} \tag{2.51}$$

where

$$\mathbf{C} = \mathbf{S}^{(1)} - \mathbf{S}^{(2)}\mathbf{D}^{(2)}(\mathbf{S}^{(4)}\mathbf{D}^{(2)} - \mathbf{D}^{(3)})^{-1}\mathbf{S}^{(3)}. \tag{2.52}$$

Once $\boldsymbol{R}$ has been determined either (2.49) or (2.50) can be manipulated to find $\boldsymbol{B}$.

Despite the apparent complexity of (2.51) it should be emphasized that the matrices $\mathbf{S}^{(i)}$, $i = 1,2,3,4$, are generally of low order, depending upon the number of modes present, $\mathbf{D}^{(i)}$, $i = 1,2,3$, are simply diagonal matrices, and $\boldsymbol{U}$ is a vector having unity as its only non-zero element.

In the case of $\lambda > 2d$, $N = M = 1$ and all matrices reduce to scalars. It is clear from (2.51) that with $\boldsymbol{R} = \{R_0\}$, $|R_0|^2 = 1$ as required from energy considerations.

The energy condition for the general case is

$$\sum_{n=-r}^{s} \alpha_n d R_n \overline{R_n} = \alpha_0 d \tag{2.53}$$

or in matrix notation

$$\boldsymbol{R}^T \mathbf{D}^{(1)} \overline{\boldsymbol{R}} = \boldsymbol{U}^T \mathbf{D}^{(1)} \boldsymbol{U}. \tag{2.54}$$

It turns out later that $\mathbf{C}^T = \overline{\mathbf{C}}$, and using (2.51) with simple matrix operations we can show that the energy conservation condition is indeed automatically satisfied.

Let us now return to (2.36), (2.37) and define

$$w_n(y) = \begin{cases} u_{n-r-1}(y), & n = 1,2,\ldots,N, \\ v_{n-N-1}(y), & n = N+1,\ldots,N+M \end{cases} \tag{2.55}$$

and

$$\chi_n(y) = \begin{cases} \Psi_{n-r-1}(y), & n = 1,2,\ldots,N, \\ \psi_{n-N-1}(y), & n = N+1,\ldots,N+M. \end{cases} \tag{2.56}$$

Then we can combine (2.36), (2.37) in the form

$$\int_{L_g} w_n(t) K(y,t) \mathrm{d}t = \chi_n(y), \quad n = 1,\ldots,N+M \tag{2.57}$$

and define the $(N+M) \times (N+M)$ matrix $\mathbf{W}$ by

$$W_{mn} = \int_{L_g} w_n(y) \overline{\chi_m(y)} \mathrm{d}y. \tag{2.58}$$

It follows that

$$\mathbf{W} = \begin{pmatrix} \mathbf{S}^{(1)} & \mathbf{S}^{(2)} \\ \mathbf{S}^{(3)} & \mathbf{S}^{(4)} \end{pmatrix}. \tag{2.59}$$

We now write (2.57) and (2.58) in operator form, thus

$$\mathscr{K} w_n = \chi_n \tag{2.60}$$

with

$$(w_n, \chi_m) = W_{mn}. \tag{2.61}$$

Since from (2.35)

$$\overline{K(y,t)} = K(t,y) \tag{2.62}$$

then

$$(u, \mathscr{K} v) = (\mathscr{K} u, v), \quad \forall u, v \tag{2.63}$$

from which it follows that

$$\boldsymbol{W}^T = \overline{\boldsymbol{W}} \tag{2.64}$$

and, from (2.52), (2.59) $\mathbf{C}^T = \overline{\mathbf{C}}$ as previously stated.

Furthermore

$$(u, \mathscr{K} u) = \sum_{n=-\infty}^{\infty}{}' (\gamma_n d)^{-1} \left| \int_{L_g} u(y) \overline{\Psi_n(y)} \mathrm{d}y \right|^2 + \sum_{n=M}^{\infty} (q_n b)^{-1} \coth q_n a \left| \int_{L_g} u(y) \psi_n(y) \mathrm{d}y \right|^2 \geqslant 0, \ \forall u(y), \tag{2.65}$$

which from (2.60), (2.61) makes it clear that W_{nn} is real and positive for $n = 1, 2, \ldots, N+M$.

Approximate solution by Galerkin method

We now seek a Galerkin approximation to (2.60) in the form $\tilde{w}_n(y) \approx w_n(y)$ such that

$$(\tilde{w}_n, \mathscr{K} \tilde{w}_n) = (\tilde{w}_n, \chi_n) = \tilde{W}_{nn}, \tag{2.66}$$

say. It follows from (2.63), (2.65) and (2.66) that

$$0 \leqslant \tilde{W}_{nn} \leqslant W_{nn} \tag{2.67}$$

and a similar result can be proved for the off-diagonal elements as shown in Porter & Evans (1995). Thus

$$|\mathrm{Re}\{\tilde{W}_{mn}\}| \leqslant |\mathrm{Re}\{W_{mn}\}| \tag{2.68}$$

and

$$|\mathrm{Im}\{\tilde{W}_{mn}\}| \leqslant |\mathrm{Im}\{W_{mn}\}|. \tag{2.69}$$

It remains to choose an appropriate expansion for the function $w_n(y)$. Now $w_n(y)$ involves u_n and v_n each of which in turn originates from the decomposition of the velocity $U(y)$ in (2.38). We shall choose $w_n(y)$ to have the same singularity at $y = 0, b$ as does $U(y)$, corresponding to the corners of the block. Thus it is easy to show that $U(y) \sim Ay^{-1/3}$ as $y \to 0$ with a similar behaviour as $y \to b$.

We thus choose

$$w_n(y) = \sum_{r=0}^{P} a_{nr} b_r(y), \quad n = 1, 2, \ldots, N+M, \tag{2.70}$$

where

$$b_r(y) = \frac{\mathrm{i}^r r! \Gamma(\frac{1}{6})}{\sqrt{2\pi} \Gamma(r + \frac{1}{3})(yb)^{1/3}(b-y)^{1/3}} C_r^{1/6}\left(\frac{2y-b}{b}\right). \tag{2.71}$$

Here $C_n^\nu(z)$ are the ultraspherical Gegenbauer polynomials given by

$$C_n^\nu(\cos\theta) = \sum_{m=0}^{n} \frac{\Gamma(\nu+m)\Gamma(\nu+n-m)}{m!(n-m)!\,[\Gamma(\nu)]^2} \cos(n-2m)\theta. \tag{2.72}$$

See, for example Abramowitz & Stegun (1972) and Erdélyi *et al.* (1954) for properties of these polynomials some of which are given in I.

Notice that each of the $b_r(y)$ has the anticipated singularity at $y = 0, b$. It should be emphasized that the choice of these polynomials and the rather curious combination of factors in (2.71) is solely to achieve simplification of the final results. See for example (2.80) and (2.81) below.

We now substitute (2.70) into (2.60), multiply by $\overline{b_m(y)}$ and integrate over L_g to obtain for $n = 1, 2, \ldots, N + M$, $m = 0, 1, \ldots, P$

$$\sum_{r=0}^{P} a_{nr} K_{mr} = H_{mn}, \tag{2.73}$$

where (2.35) has been used for

$$\begin{aligned} K_{mn} &= (\mathscr{K} b_n, b_m) \\ &= {\sum_{r=-\infty}^{\infty}}' \frac{1}{\gamma_r d} G_{mr} \overline{G_{nr}} + \sum_{r=M}^{\infty} \frac{\coth(q_r a)}{q_r b} F_{mr} \overline{F_{nr}} \end{aligned} \tag{2.74}$$

and

$$\begin{aligned} H_{mn} &= (\chi_n, b_m) \\ &= \begin{cases} G_{m,n-r+1}, & n = 1, 2, \ldots, N, \\ F_{m,n-N-1}, & n = N+1, \ldots, N+M, \end{cases} \end{aligned} \tag{2.75}$$

where

$$G_{mn} = (\Psi_n, b_m) = \int_{L_g} \Psi_n(y) \overline{b_m(y)} \mathrm{d}y \tag{2.76}$$

and

$$F_{mn} = (\psi_n, b_m) = \int_{L_g} \psi_n(y) \overline{b_m(y)} \mathrm{d}y. \tag{2.77}$$

Also substituting (2.70) into (2.61) we find

$$W_{mn} = \sum_{r=0}^{P} a_{nr} \overline{H_{rm}}. \tag{2.78}$$

It can be shown using results stated in I that

$$\overline{F_{m0}} = \frac{6}{2^{1/6} \Gamma(\frac{1}{6})} \delta_{m0}, \tag{2.79}$$

and

$$\overline{F_{mn}} = \varepsilon_n^{1/2} \, \mathrm{i}^m \cos \frac{\pi}{2}(m+n) \left(\frac{2}{n\pi}\right)^{1/6} J_{m+1/6}\left(\frac{n\pi}{2}\right), \tag{2.80}$$

whilst

$$\overline{G_{mn}} = \mathrm{e}^{-\mathrm{i}\beta_n b/2} \left(\frac{2}{\beta_n b}\right)^{1/6} J_{m+1/6}\left(\frac{\beta_n b}{2}\right). \tag{2.81}$$

Note that in I, $0 < \beta_0 d < \pi/2$ and thus $\overline{G_{mn}}$ kept the same form for all m, n. Here this is not so (for example the case of normal incidence is $\beta_0 d = 0$). In general it can be shown that if any $\beta_n b = 0$ then (2.81) becomes $\overline{G_{mn}} = 6\delta_{m,0}/2^{1/6}\Gamma(1/6)$.

Thus from (2.74), (2.79)–(2.81),

$$K_{mn} = \sum_{r=-\infty}^{\infty}{}' \frac{1}{\gamma_r d}\left(\frac{2}{\beta_r b}\right)^{1/3} J_{m+1/6}\left(\frac{\beta_r b}{2}\right) J_{n+1/6}\left(\frac{\beta_r b}{2}\right) + \sum_{r=M}^{\infty} P_{rmn}\frac{\coth q_r a}{q_r b}\left(\frac{2}{\pi r}\right)^{1/3} J_{m+1/6}\left(\frac{r\pi}{2}\right) J_{n+1/6}\left(\frac{r\pi}{2}\right) \tag{2.82}$$

where

$$P_{rmn} = \tfrac{1}{2}\{(-1)^r + (-1)^m\}\{(-1)^r + (-1)^n\} \tag{2.83}$$

which shows that the K_{mn} are real. Using this fact we can show from (2.73), (2.78) that

$$\boldsymbol{W} = \bar{\boldsymbol{a}}\boldsymbol{K}\boldsymbol{a}^T \tag{2.84}$$

in an obvious matrix notation.

This completes the solution for the symmetric functions ϕ_s. A similar procedure is necessary for the antisymmetric function ϕ_a. The only major changes are that in the final formulation coth is replaced by tanh in K_{mn} in (2.82), and $\boldsymbol{D}^{(2)}$ in (2.44) and $\boldsymbol{D}^{(3)}$ in (2.45) are replaced by $\boldsymbol{D}^{(2)} = \mathrm{diag}\{-\mathrm{i}\sin(k_n a)\}$ and $\boldsymbol{D}^{(3)} = \mathrm{diag}\{\mathrm{i}k_n b\sin(k_n a)\}$, respectively.

If we re-label the R_n from the ϕ_s solution as R_n^s and those obtained from the ϕ_a solution as R_n^a we can obtain overall reflection and transmission coefficients since from (2.19), (2.21)

$$\phi(x,y) \sim \mathrm{e}^{-\mathrm{i}\alpha_0(x-a)}\Psi_0(y) + \frac{1}{2}\sum_{n=-r}^{s}(R_n^s + R_n^a)\mathrm{e}^{\mathrm{i}\alpha_n(x-a)}\Psi_n(y) \quad \text{as } x \to +\infty, \tag{2.85}$$

$$\phi(x,y) \sim \frac{1}{2}\sum_{n=-r}^{s}(R_n^s - R_n^a)\mathrm{e}^{-\mathrm{i}\alpha_n(x+a)}\Psi_n(y) \quad \text{as } x \to -\infty, \tag{2.86}$$

Thus we can define the overall reflection and transmission coefficients R_n and T_n as

$$R_m = \tfrac{1}{2}(R_n^s + R_n^a) \quad \text{and} \quad T_n = \tfrac{1}{2}(R_n^s - R_n^a). \tag{2.87}$$

Finally using the fact that the energy conservation condition (2.53) for the symmetric and antisymmetric solutions is automatically satisfied, it is not difficult to show that the total energy condition for the whole problem which can be written in the form

$$\sum_{n=-r}^{s}\frac{\alpha_n}{\alpha_0}\left\{|R_n|^2 + |T_n|^2\right\} = 1 \tag{2.88}$$

is also automatically satisfied.

3. Results

We seek to compute the reflection and transmission properties of the periodic array of rectangular blocks. Given the angle of incidence of the incoming wave field θ_0, the wavenumber $k = 2\pi/\lambda$ related to the frequency of motion $\omega/2\pi$ by (2.2), and a particular geometry determined from a, b and d, we first find the number of reflected and transmitted modes R_n and T_n $(-r \leqslant n \leqslant s)$ given by $N = r + s + 1$ where r and s are determined from (2.15) and (2.16). Since we have separated the problem into symmetric and antisymmetric parts we have to find the two sets of solutions

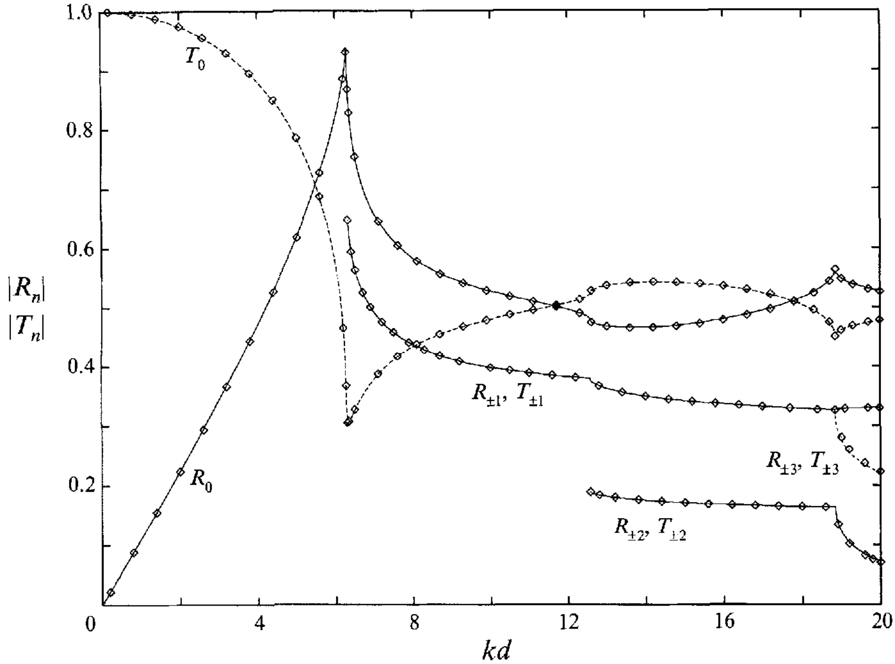

FIGURE 2. $|R_n|$, $|T_n|$ against kd where $\theta_0 = 0$, $a/d = 0.0001$ and $b/d = 0.5$. Also shown (using diamond symbols) are results from Porter & Evans (1995) for the vertical plates.

determining $R_n^{(s,a)}$ in order to calculate R_n and T_n from (2.87). In each case we first have to choose P trial functions $b_r(y)$ and then calculate a_{nr} from the system (2.73) which depends on K_{mn} given by (2.82) and (2.83). Note that for large r the r^{th} term of each of the series in (2.82) is $O(r^{-7/3})$ and this is sufficient for K_{mn} to be computed to any desired accuracy as a function of all the input parameters θ_0, k, a, b and d. In practice $r = 500$ was generally sufficient to give at least three-figure accuracy in the elements K_{mn}. Once the a_{nr} have been calculated the matrix $\boldsymbol{W}$ is calculated from either (2.84) or (2.78) and thus the matrices $\boldsymbol{S}^{(i)}$, $i = 1, 2, 3, 4$ by (2.59). The reflection vector $\boldsymbol{R}$ is then determined from (2.51) and (2.52), from which $R_n^{(s,a)}$, $-r \leqslant n \leqslant s$ are found after applying the appropriate changes to the formulation for symmetric and antisymmetric solutions. Convergence of $\boldsymbol{R}$ with increasing P proves to be extremely rapid, with the final forms for R_n, T_n converging to at least three significant figures for $P \geqslant 5$.

The number of parameters in the problem is large and many possibilities exist for presentation of the results. We shall begin by comparing our results with the known exact numerical results of Porter & Evans (1995) who used complementary bounds to obtain results for scattering properties of periodic in-line thin barriers. It is clearly not possible to put $a/d = 0$ in our formulation. However in figure 2 we have plotted the modulus of the reflection and transmission coefficients against the non-dimensionalized wavenumber kd for the case of normal incidence $\theta_0 = 0$, $b/d = 0.5$ and $a/d = 0.0001$. We see that the higher modes start to appear at multiples of 2π ($kd = 2n\pi, n = 1, 2, \ldots$) and that $|R_{\pm n}| = |T_{\pm n}|$ for $n \geqslant 1$. Also shown using diamond symbols are values calculated from Porter & Evans (1995) for the same case. We see from the figure that the results agree extremely well.

Another comparison of results is made in figure 3 where $|R_0|$ is plotted against

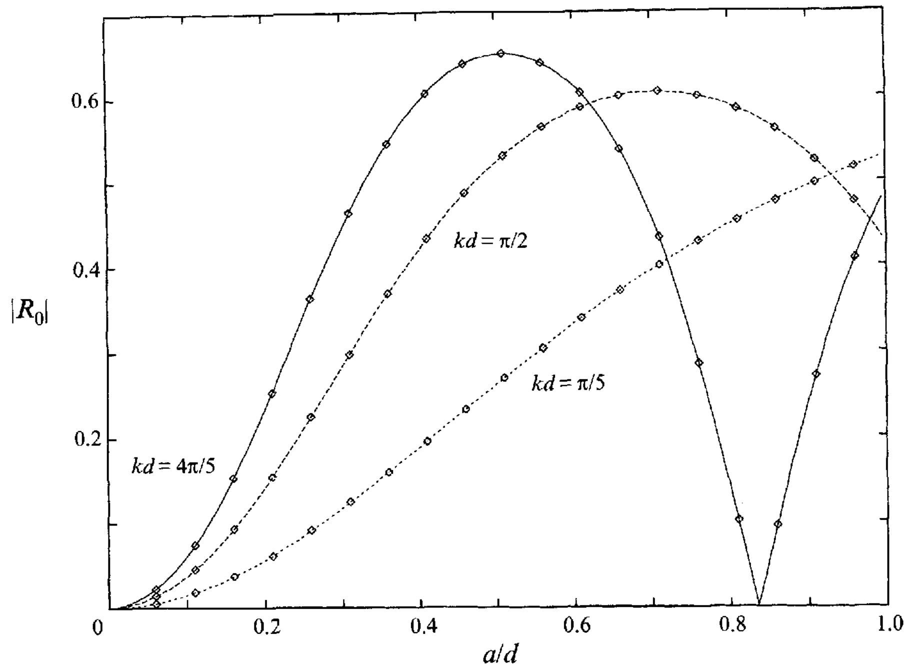

FIGURE 3. $|R_0|$ against a/d for various values of kd where $\theta_0 = 2\pi/3$, $b/d = 1.0$. Also shown (using diamond symbols) are results from Linton & Evans (1993) for the parallel plates.

a/d for various values of kd ($= 4\pi/5$, $\pi/2$, $\pi/5$) when $\theta_0 = 2\pi/3$ and $b/d = 1.0$. These results correspond to the scattering by an array of parallel plates and as we can see these results also agree extremely well with the results of Linton & Evans (1993*a*, figure 2) (shown using diamond symbols) obtained for this geometry using a technique based on residue calculus. In the previous figure we could not set $a/d = 0$ identically because of the formulation of the problem, but in this case b/d can be set exactly to 1 without having to take a numerical limit. We also see in figure 3 that we have a zero of reflection when $kd = 4\pi/5$ at approximately $a/d = 0.83$.

In the formulation of the Galerkin approximation we 'built in' the required $O(r^{-1/3})$ singularity as we approach the corners of the blocks, but for the case when we 'squash' the blocks into vertical and parallel plates the singularity is now $O(r^{-1/2})$ at the end of the plates. It is still remarkable how good the agreement is despite this difference in singularities.

In figure 4 we have plotted $|R_0|$ and $|T_0|$ against θ_0 for two cases where the blocks are of square cross-section for $kd = 1.0$, (*a*) $a/d = 0.1768$, $b/d = 0.6464$ and (*b*) $a/d = 0.25$, $b/d = 0.5$. We see that we have total reflection for both cases. Also plotted with symbols are results obtained by Linton & Evans (1993*b*, figure 3*a*) for the scattering by a periodic array of circular cylinders. These values have been chosen so that (*a*) the blocks fit exactly inside the cylinders and (*b*) the cylinders fit exactly inside the blocks. We see that in both cases the cylinder reflects less of the incoming wave field over most angles of incidence, suggesting that the shape of obstacles is important in determining the amount of reflection and transmission.

In figure 5, $|R_0|$ is plotted against θ_0 for various values of b/d, and $kd = 1.0$. For all these values only one travelling mode exists. The first thing to note is that as $\theta_0 \to \pi/2$, $|R_0| \to 1$ which is what one would expect as the incident field travels parallel to the array of blocks. We also see that at normal incidence ($\theta_0 = 0$) the

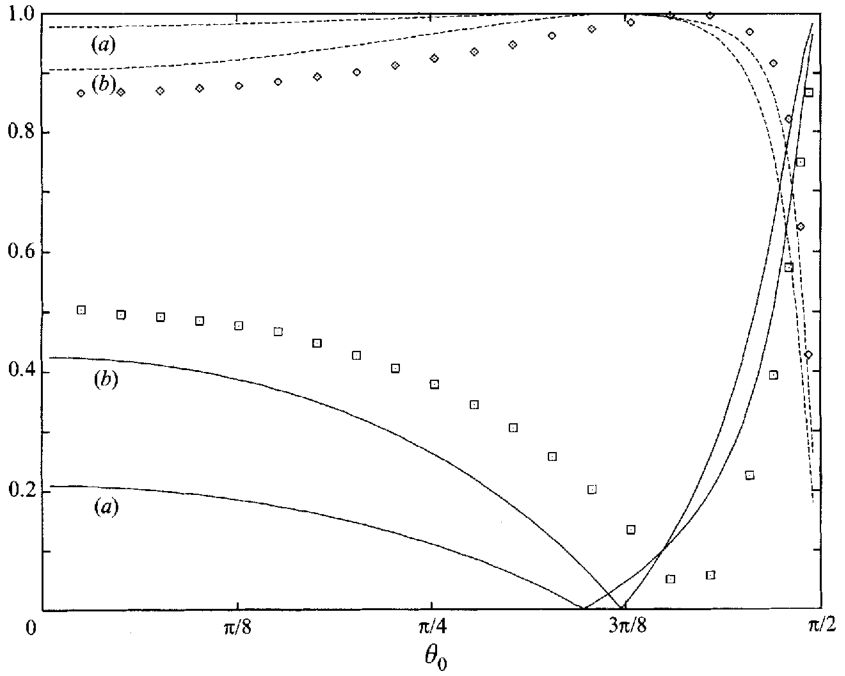

FIGURE 4. $|R_0|$, $|T_0|$ against θ_0 (——, $|R_0|$; – – –, $|T_0|$) where $kd = 1.0$ with (a) inner square $a/d = 0.1768$, $b/d = 0.6464$; (b) outer square $a/d = 0.25$, $b/d = 0.5$. Also shown by the square and diamond symbols are $|R_0|$, $|T_0|$ for circular cylinders by Linton & Evans (1993b).

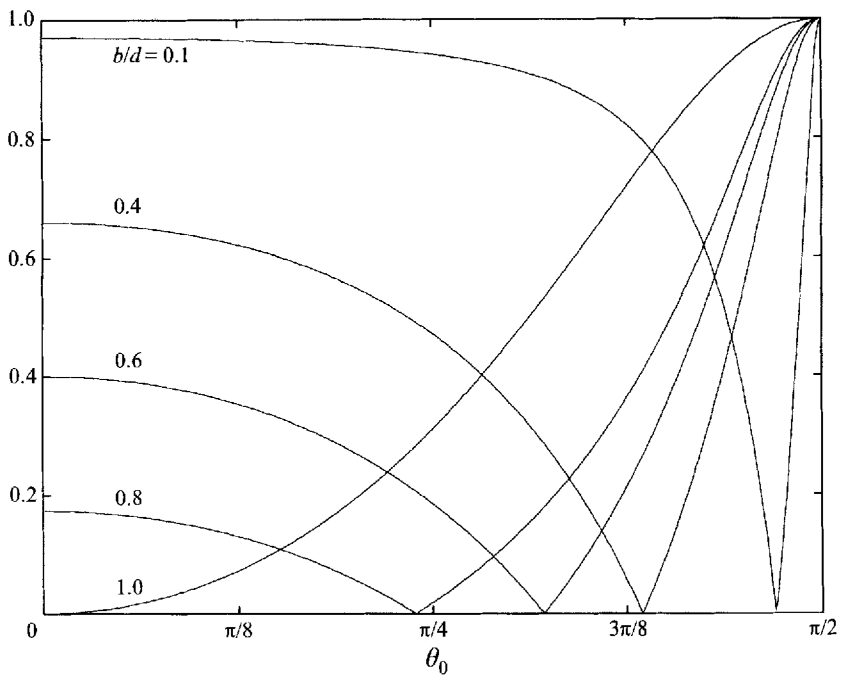

FIGURE 5. $|R_0|$ against θ_0 for various values of b/d where $a/d = 0.4$, $kd = 1.0$.

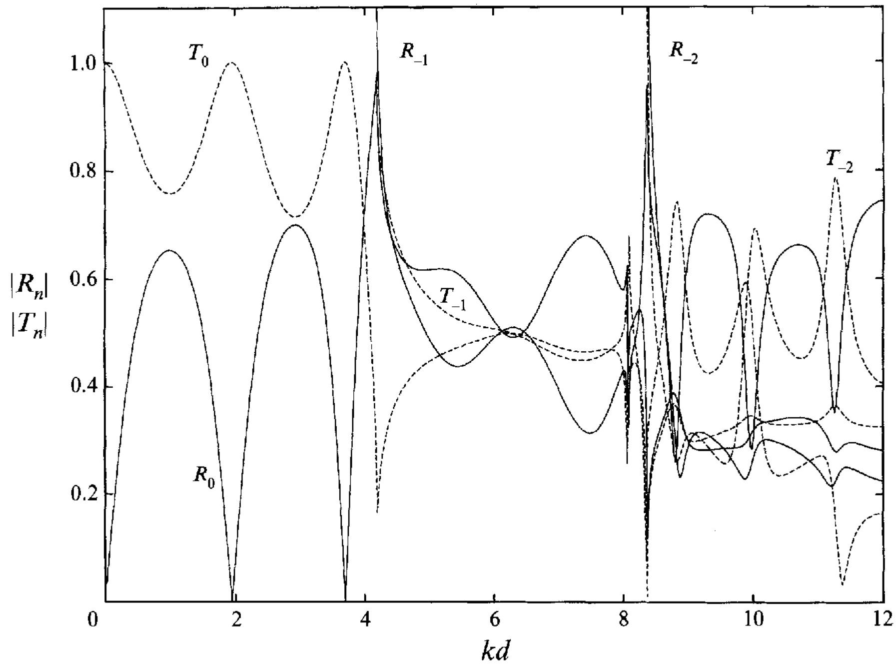

FIGURE 6. $|R_n|$ and $|T_n|$ against kd where $a/d = 0.7$, $\theta_0 = \pi/6$ and $b/d = 0.4$.

larger the gap (b/d) the less reflection we have and as $b/d \to 0$, the reflection increases as expected. Note also that complete transmission ($|R_0| = 0$) of the incident wave occurs at larger angles as the gap size (b/d) decreases.

In general as kd is increased more travelling modes occur and the graphs produced for $|R_n|$ and $|T_n|$ become more complicated. A typical example is shown in figure 6 for the case $a/d = 0.7$, $b/d = 0.4$ and $\theta_0 = \pi/6$. Before the first cut-off, $kd < 4\pi/3$, there exists two zeros of reflection and as we pass the first cut-off the second set of travelling modes appears. Note that $|R_{-1}| > 1$ (≈ 1.22) although the energy condition (2.88) is still satisfied. Again another set of travelling modes appears at $kd > 8\pi/3$ with $|R_{-2}| \approx 1.60$.

Because of the very complicated behaviour of the reflection and transmission coefficients as higher modes appear it is more illuminating to consider the total transmitted wave energy through the array of rectangular blocks as a proportion of the incident wave energy. This quantity is also calculated in Porter & Evans (1995) and is given by

$$T_{total} = \sum_{n=-r}^{s} \frac{\alpha_n}{\alpha_0} |T_n|^2.$$

In figure 7 we have plotted T_{total} against θ_0 for four cases, $b/d = 0.1, 0.4, 0.6, 0.8$, where $a/d = 0.4$ and $kd = 5.0$. We see that below the cut-off at $\theta_0 = \sin^{-1}(2\pi/5 - 1)$ (≈ 0.260) the larger b/d, the larger T_{total} as expected, but as θ_0 increases beyond $\theta_0 \approx 1.39$ this behaviour is reversed.

In figure 8 T_{total} is plotted against kd for various θ_0 and for $a/d = 0.1$ and $b/d = 0.4$. Notice that there appears to be total reflection for $\theta_0 = 0$ at $kd = 2\pi$. However this would be masked in reality by the proximity of the occurrence of zero reflection at a slightly lower value of θ_0. It is clear that using a periodic array of blocks as a

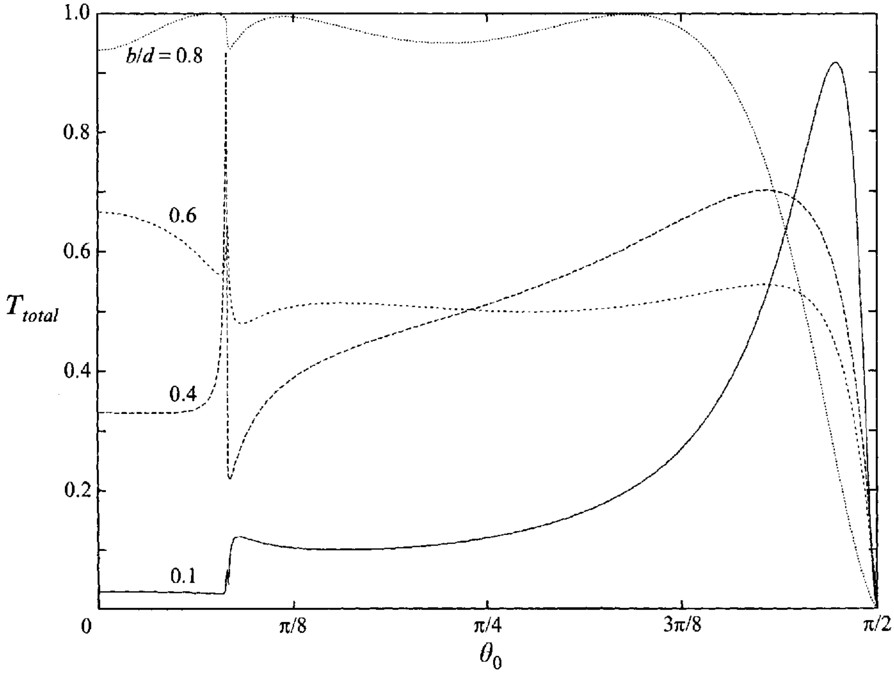

FIGURE 7. T_{total} against θ_0 for various values of b/d where $a/d = 0.4$, $kd = 5.0$.

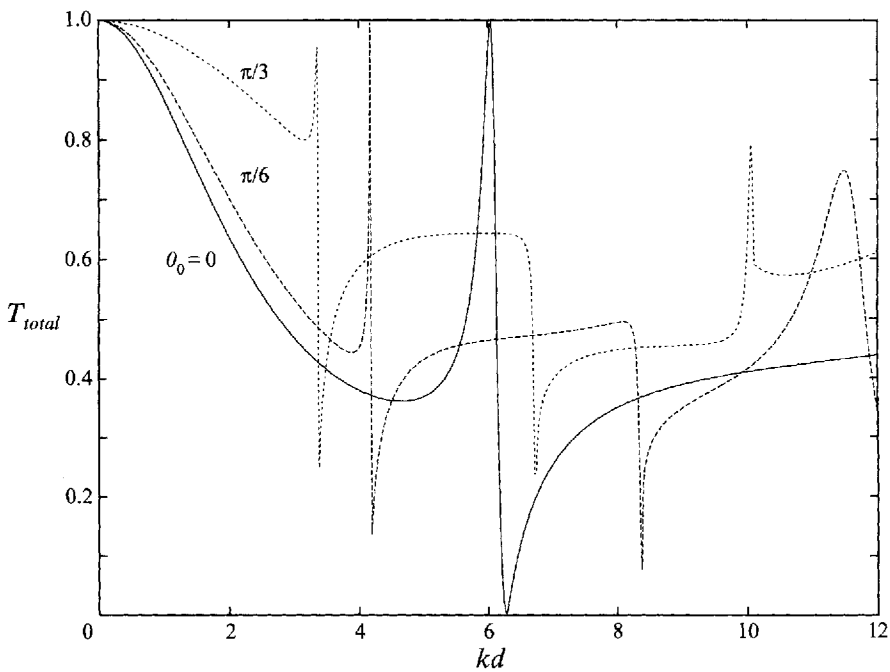

FIGURE 8. T_{total} for various θ_0 against kd where $a/d = 0.1$ and $b/d = 0.4$.

breakwater, whilst being effective in certain parameter ranges, can also produce large amounts of transmission through interference effects.

4. Conclusion

In this paper, a technique based on ideas developed in Evans & Fernyhough (1995) has been given for numerically calculating the reflection and transmission coefficients for the problem of scattering by a periodic array of rectangular blocks. By using a matrix formulation the full multi-modal scattering was able to be considered and the problem was reduced to the solution of a set of integral equations to which a Galerkin approach was applied involving the use of ultra-spherical Gegenbauer polynomials as trial function expansions.

The solution obtained proved to be extremely accurate and numerically efficient for all parameters and gave good agreement with the results of Porter & Evans (1995) and Linton & Evans (1993*a*) for in-line or parallel plates.

REFERENCES

Abramowitz, M. & Stegun, I. A. 1972 *Handbook of Mathematical Functions*, 9th Edn. Dover.

Achenbach, J. D. & Li, Z. L. 1986 Reflection and transmission of scalar waves by a periodic array of screens. *Wave Motion* **8**, 225–234.

Dalrymple, R. A. & Martin, P. A. 1990 Wave diffraction through offshore breakwaters. *J. Waterway, Port, Coastal Ocean Engng* **116**, 727–741.

Erdélyi, A., Magnus, Oberhettinger, W., F. & Tricomi, F. G. 1954 *Tables of Integral Transforms.* Bateman manuscript project, vol. 1. McGraw-Hill.

Evans, D. V. & Fernyhough, M. 1995 Edge waves along periodic coastlines. Part 2. *J. Fluid Mech.* **297**, 307–325 (referred to herein as I).

Kristiansen, U. R. & Fahy, F. J. 1972 Scattering of acoustic waves by and N-layer periodic grating. *J. Sound Vib.* **24**, 315–335.

Linton, C. M. & Evans, D. V. 1993*a* Acoustic scattering by an array of parallel plates. *Wave Motion* **18**, 51–65.

Linton, C. M. & Evans, D. V. 1993*b* The interaction of waves with a row of circular cylinders. *J. Fluid Mech.* **251**, 687–708.

Mongeau, L., Amram, M. & Rousselet, J. 1986 Scattering of sound waves by a periodic array of slotted waveguides. *J. Acoust. Soc. Am.* **80**, 665–671.

Petit, R. 1980 *Electromagnetic Theory of Gratings, Topics in Current Physics.* Springer.

Porter, R. & Evans, D. V. 1995 Wave scattering by periodic arrays of breakwaters. *Wave Motion* (to appear).

Wilcox, C. H. 1984 *Scattering Theory for Diffraction Gratings.* Springer.

Williams, A. N. & Crull, W. W. 1993 Wave diffraction by thin screen breakwaters. *J. Waterway, Port, Coastal Ocean Engng* **119**, 606–617.